VELOCITY AND PRESSURE MEASUREMENTS ON A BROAD-CRESTED WEIR: PHYSICAL MEASUREMENTS

S. Felder[1] and H. Chanson[1]

[1]University of Queensland, School of Civil Engineering, Brisbane QLD 4072, Australia,
h.chanson@uq.edu.au

Abstract: Basic experiments were conducted on a large-size broad-crested weir with an upstream rounded corner. Detailed velocity and pressure measurements were performed for a range of flow conditions. The results showed the rapid flow re-distribution at the upstream end of the weir, as well as next to the weir brink at large flow rates. Assuming non-uniform velocity and non-hydrostatic pressure distributions, it is shown that critical flow conditions were achieved above the whole crest length. The velocity measurements highlighted a developing boundary layer. The data differed from the smooth turbulent boundary layer theory, although the present results were consistent with earlier studies.

Keywords: broad-crested weir, velocity and pressure distributions, critical flow conditions, turbulent boundary layer.

INTRODUCTION

A broad-crested weir has a relatively long and flat crest for the streamlines to be parallel to the crest profile and the pressure distribution be hydrostatic (Bos 1976, Montes 1998). The discharge above the weir is typically estimated as:

$$Q = C_D \times \sqrt{g \times \left(\frac{2}{3} \times H_1\right)^3} \times B \quad (1)$$

where Q is the flow rate, B the channel width, g the gravity acceleration, H_1 is the upstream total head above crest, and C_D the discharge coefficient (Henderson 1966, Chanson 2004). Bélanger (1841) analysed theoretically the overflow and derived Equation (1) for the ideal case (C_D = 1). Successful physical studies included Bazin (1896), Woodburn (1932), Tison (1950), Serre (1953), Ramamurthy et al. (1988) and Gonzalez and Chanson (2007).

It is the aim of this paper to detail the pressure and velocity profiles on a broad-crested weir with rounded corner. New physical data provide a better understanding of the pressure and velocity redistributions on the broad-crest, including the boundary layer development.

PHYSICAL STUDY AND INSTRUMENTATION

The experiments were conducted in a 7 m long, 0.52 m wide test section (Fig. 1). Waters were supplied in a 1.5 m deep intake basin leading to a profiled sidewall convergent with a 4.2:1

contraction ratio to enable a smooth waveless inflow into the test section. The weir was 1 m high, 0.52 m wide with a 1.01 m long flat horizontal crest designed with an upstream rounded corner (0.080 m radius) and a downstream sharp corner (Fig. 1).

A recirculation pump supplied the flow rate through a closed-circuit system. The water depths were measured on the channel centreline using point gauges and sidewall photography undertaken with dSLR cameras. The point gauge and photographic data yielded identical results within 0.5 mm. Pressure and velocity measurements were performed with a Prandtl-Pitot tube (Ø = 3.0 mm). The translation of the Pitot-Prandtl probe in the vertical direction was controlled by a fine adjustment travelling mechanism. The error on the vertical position of probe was less than 0.25 mm. The accuracy on longitudinal position was estimated ± 1 mm while the error on the probe transverse position was less than 1 mm.

Fig. 1 - Photographs of the free-surface at the downstream end of weir crest (i.e. brink) for H_1/L_{crest} = 0.18 (Top) and 0.24 (Bottom) with flow direction from left to right - Note the Prandtl-Pitot tube on the right

BASIC RESULTS

The free-surface upstream of and above the crest was very smooth for all investigated discharges ($0.0025 < Q < 0.142$ m^3/s). Immediately upstream of the weir crest, the flow was accelerated, became critical above the crest (see below) and was supercritical on the downstream steep slope (Fig. 1 & 2). Figure 1 shows some photographs of the free-surface and Figure 2 presents some

typical free-surface profiles where d is the flow depth and L_{crest} is the crest length. The data showed that the free-surface was not horizontal as previously reported (Woodburn 1932). For some flow rates, a wavy profile was observed above the crest: e.g., for H_1/L_{crest} = 0.06 and 0.10 in Figure 2. These might be linked with the interactions between developing boundary layer and main flow (Isaacs 1981).

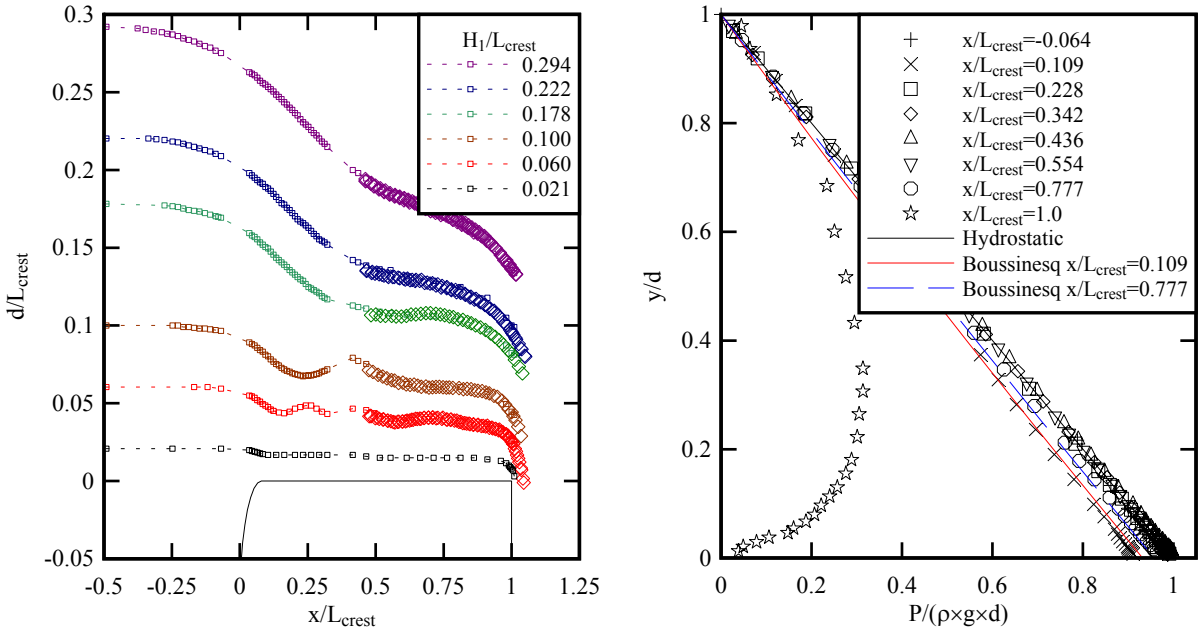

Fig. 2 (Left) - Free-surface profiles above a broad-crested weir: point gauge (small squares & dashed line) and photographic (empty diamonds) data

Fig. 3 (Right) - Pressure distributions along the broad-crested weir for H_1/L_{crest} = 0.224 - Comparison with the hydrostatic pressure and a Boussinesq equation solution for x/L_{crest} = 0.109 & 0.777

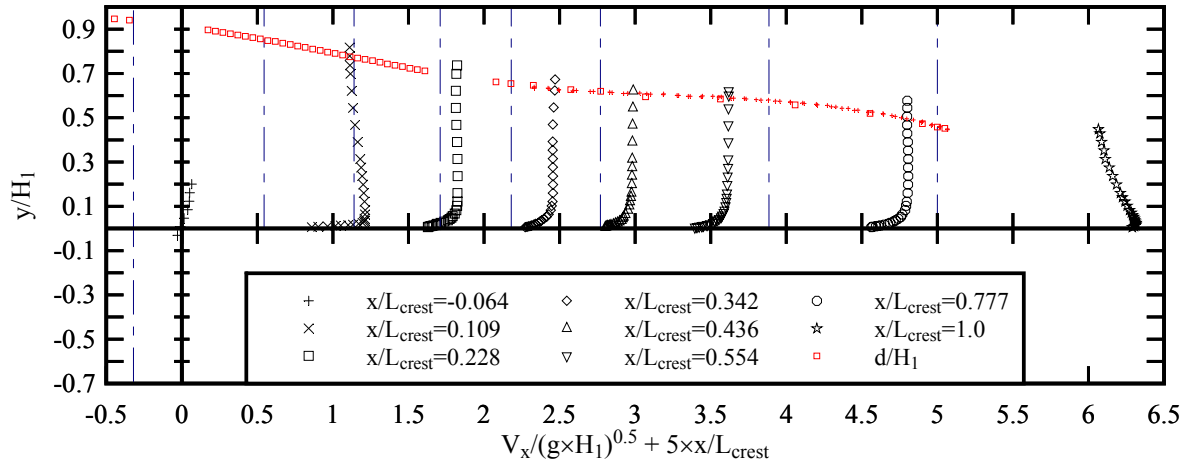

Fig. 4 - Velocity distributions along the broad-crested weir for H_1/L_{crest} = 0.218 - Free-surface data shown with red symbols

Some typical velocity and pressure distributions are shown in Figures 3 & 4. In Figure 3 the pressure distributions are compared with the hydrostatic profile, as well as with an analytical solution of Boussinesq equation at x/L_{crest} = 0.11 & 0.78 (Montes and Chanson 1998), calculations being based upon free-surface curvature observations. The velocity and pressure distributions data showed consistently some rapid redistribution of pressure and velocity fields at both upstream and downstream ends of the broad crest (Fig. 3 & 4): i.e., the flow there was rapidly-varied. For x/L_{crest} < 0.2, the pressure gradient was typically less hydrostatic, and the velocity profile had a shape close to that predicted by the ideal fluid flow theory. At the downstream end, the free-surface curvature became pronounced as the flow accelerated near the brink (Fig. 1). Namely the velocity and pressure fields at the brink were similar to those observed at a free overfall (Henderson 1966) (Fig. 3 & 4).

The rapid flow redistribution at the upstream end of weir crest was associated with the development of a turbulent boundary layer. The no-slip condition at the invert (y = 0) induced a turbulent boundary layer growth. The boundary layer development was estimated from the measured velocity profiles. For the present data set, the growth of boundary layer thickness was best correlated by:

$$\frac{\delta}{x} \sim \left(\frac{x}{k_s}\right)^{-0.124} \qquad x/L_{crest} < 0.7 \quad (2)$$

where δ is the boundary layer thickness defined in terms of 99% of the free-stream velocity, x the distance along the crest and k_S the equivalent sand roughness height (herein k_S = 0.5 mm). The boundary layer growth was about $\delta \sim x^{0.87}$ compared to a smooth turbulent boundary layer growth of $\delta \sim x^{0.8}$ (Schlichting 1979, Chanson 2009).

The boundary layer data showed further an apparent reduction in boundary layer thickness at the downstream end of the crest for the larger discharges. It is believed to be associated with some velocity redistributions induced by the streamline curvature. Such a flow redistribution was documented by Vierhout (1973) and Matos (2011, Pers. Comm.).

CRITICAL FLOW CONDITIONS AND DISCHARGE COEFFICIENT

Above the broad crest, the specific energy is minimum and critical flow conditions do take place. While the free surface was not parallel to the crest herein, the depth-averaged specific energy was constant along the crest (data not shown). The depth-averaged specific energy H above the crest is commonly expressed following Liggett (1993) and Chanson (2006):

$$H = \frac{1}{d} \times \int_0^d \left(\frac{{v_x}^2}{2 \times g} + z + \frac{P}{\rho \times g}\right) \times dz = \beta \times \frac{V^2}{2 \times g} + \Lambda \times d \quad (3)$$

where P the pressure, V the depth-averaged velocity, v_x the longitudinal velocity component, z the vertical elevation above the crest, β the Boussinesq momentum correction coefficient, and Λ a pressure correction coefficient:

$$\Lambda = \frac{1}{2} + \frac{1}{d} \times \int_0^d \frac{P}{\rho \times g \times d} \times dy \quad (4)$$

For an uniform flow above a flat broad crest with streamlines parallel to the crest, the velocity distribution is uniform ($\beta = 1$), the pressure is hydrostatic ($\Lambda = 1$), and Equation (3) equals the classical result: $H = 1.5 \times d_c$ where d_c is the critical flow depth. In practice, the velocity distributions were not uniform along the crest because of boundary friction and the streamlines were not parallel to the crest everywhere (Fig. 2, 3 & 4).

When the specific energy is minimum, the flow conditions above the crest are critical (Bakhmeteff 1932, Henderson 1966) and the flow depth d must satisfy one of four physical solutions (Chanson 2006):

$$\frac{d}{H} \times \Lambda = \sqrt[3]{\frac{1 - 2 \times \beta \times {C_D}^2 \times \Lambda^2}{27} + \Lambda^3 \times \sqrt{\Delta}} + \sqrt[3]{\frac{1 - 2 \times \beta \times {C_D}^2 \times \Lambda^2}{27} - \Lambda^3 \times \sqrt{\Delta}} + \frac{1}{3} \qquad \Delta > 0 \text{ (5a)}$$

$$\frac{d}{H} \times \Lambda = \frac{2}{3} \qquad \Delta = 0 \text{ (5b)}$$

$$\frac{d}{H} \times \Lambda = \frac{2}{3} \times \left(\frac{1}{2} + \cos\frac{\varepsilon}{3} \right) \qquad \Delta < 0, \text{ Solution S1 (5c)}$$

$$\frac{d}{H} \times \Lambda = \frac{2}{3} \times \frac{1 - \cos\frac{\varepsilon}{3} + \sqrt{3 \times \left(1 - \left(\cos\frac{\varepsilon}{3} \right)^2 \right)}}{2} \qquad \Delta < 0, \text{ Solution S3 (5d)}$$

where $\cos\varepsilon = 1 - 2 \times \beta \times {C_D}^2 \times \Lambda^2$ and the discriminant Δ equals:

$$\Delta = \frac{4 \times \beta \times {C_D}^2 \times \Lambda^2}{(3 \times \Lambda)^6} \times (\beta \times {C_D}^2 \times \Lambda^2 - 1) \qquad (6)$$

Equation (5) expresses the flow depth at critical flow conditions in the general case when $\beta > 1$ and $\Lambda \neq 1$. The present experimental data were tested against Equation (5) and shown in Figure 5 with the dimensionless water depth $d \times \Lambda / H_1$ being a function of the dimensionless discharge coefficient $\beta \times {C_D}^2 \times \Lambda^2$, where β and Λ were calculated based upon the pressure and velocity distribution data and C_D was estimated using Equation (1) using a discharge per unit width deduced from the mass conservation equation:

$$\frac{Q}{B} = \int_0^d v_x \times dy \qquad (7)$$

In Figure 5, each data set regroups the flow depth measurements for $0.1 < x/L_{crest} < 1$, and the results are compared with experimental data obtained above circular crested weirs and in undular flows. The present data set showed a good agreement with the theory along the entire weir crest, in particular with the solutions S1 and S3 ($\Delta < 0$) (Fig. 5). The agreement between Equation (5) and data highlighted that the assumption of critical flow conditions holds along the crest ($0.1 < x/L_{crest} < 1$) despite the boundary layer development and the non-horizontal free-surface.

The present data in terms of discharge coefficient C_D are presented in Figure 6. They showed a slight increase in discharge coefficient with increasing head above crest similar to earlier data sets. For large dimensionless heads above crest, the weir would no longer act as broad-crest, and the discharge coefficient would tend to values close to those observed on circular weirs and ogee crests.

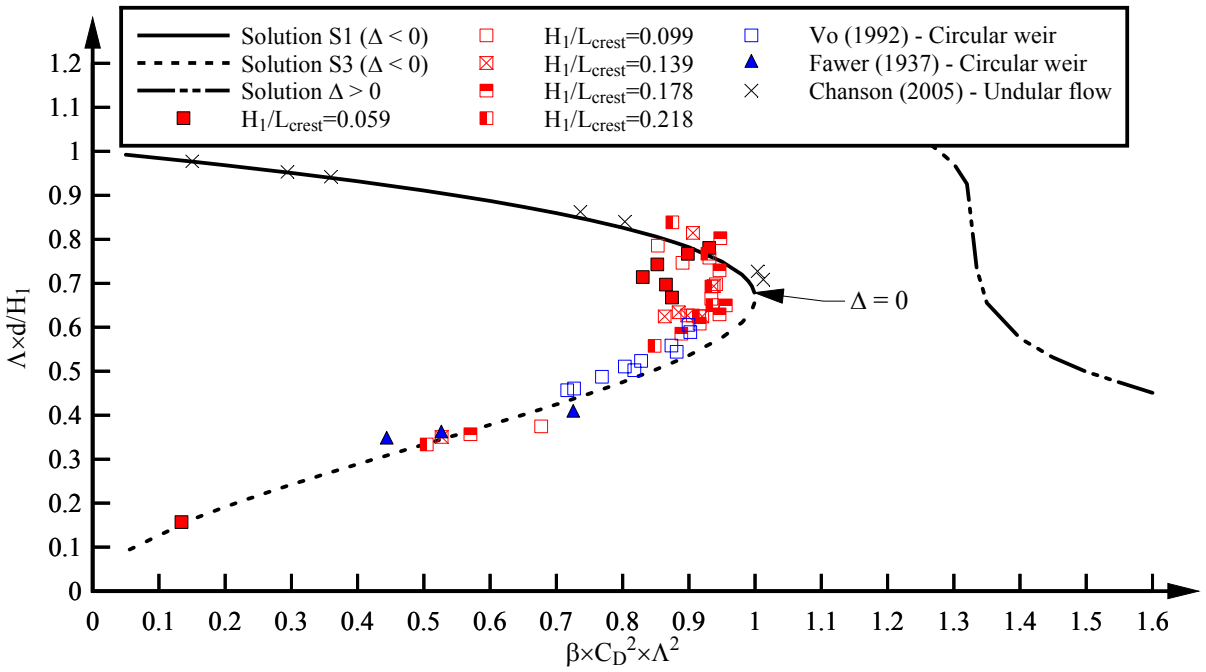

Fig. 5 - Dimensionless flow depth above the weir crest $d \times \Lambda / H_1$ as a function of the discharge coefficient $\beta \times C_D^2 \times \Lambda^2$ - Comparison between broad-crested weir data (Present study, $0.1 < x/L_{crest} < 1$), analytical solutions (Eq. (5)), circular crested weir data (Fawer 1937, Vo 1992) and undular flow data (Chanson 2005)

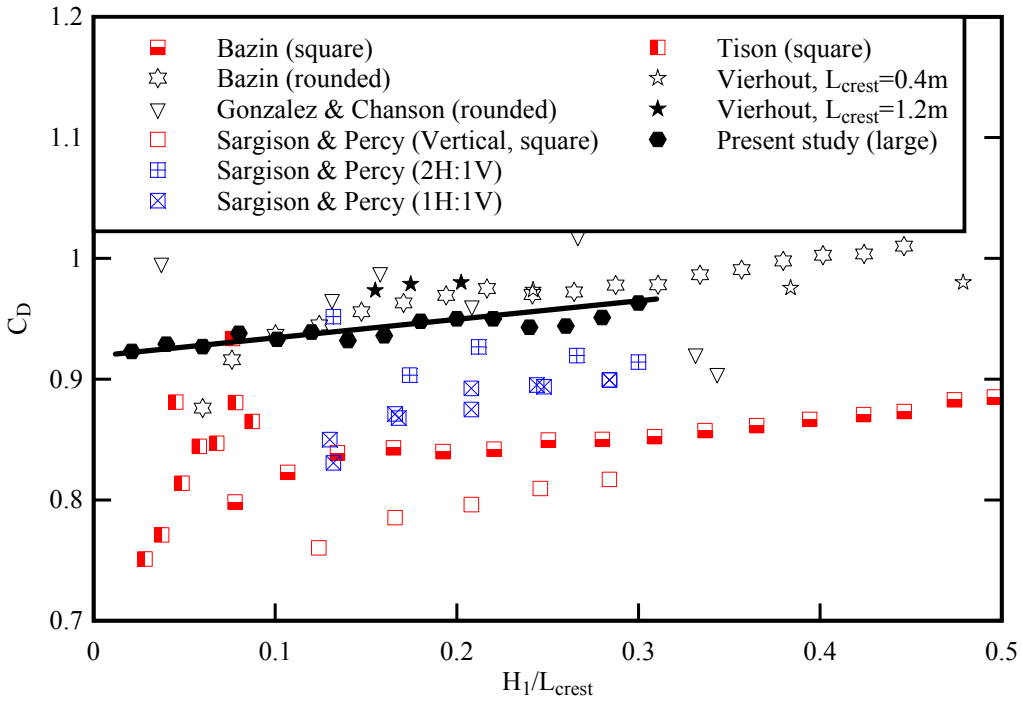

Fig. 6 - Dimensionless discharge coefficients C_D for broad-crested weirs with square corner (red symbols), inclined upstream wall (blue symbols) and rounded corner (back symbols) - Comparison with Equation (8)

Overall the dimensionless discharge coefficient data was best correlated by:

$$C_D = 0.92 + 0.153 \times \frac{H_1}{L_{crest}} \qquad \text{Present study (8)}$$

for $0.02 < H_1/L_{crest} < 0.3$. Equation (8) is shown in Figure 6. Note that the present data trend differed from the data of Gonzalez and Chanson (2007) who observed the occurrence of corner eddies next to the sidewalls immediately upstream of the vertical upstream wall, associated with instabilities affecting the overflow motion.

CONCLUSION

Some new physical experiments were conducted on a large broad-crested weir with a rounded corner. The pressure and velocity distributions were measured for a wide range of flow conditions within $0.02 < H_1/L_{crest} < 0.3$. The results highlighted the rapid redistributions of velocity and pressure fields at both upstream and downstream ends of the crest, although the flow was critical along the crest. At the upstream end, the flow motion was irrotational and the pressure and velocity distributions were affected by the streamline and free-surface curvature. At the downstream end of the crest, the flow properties were close to those observed at an overfall brink. The velocity distributions measurements highlighted a developing boundary layer. While the data differed from the smooth turbulent boundary layer theory, the results were consistent with earlier studies. The dimensionless discharge coefficient C_D was close to earlier results with rounded broad crests and C_D was typically larger than for square broad crests.

ACKNOWLEDGMENTS

The writers thank Ahmed Ibrahim and Jason Van Der Gevel (The University of Queensland) for the technical assistance. The financial support of the Australian Research Council (Grant DP0878922) is acknowledged. The first author was supported by an University of Queensland research scholarship.

REFERENCES

Bakhmeteff, B.A. (1932). *Hydraulics of Open Channels.* McGraw-Hill, New York, USA, 1st ed., 329 pages.

Bazin, H. (1896). *Expériences Nouvelles sur l'Ecoulement par Déversoir*. ('Recent Experiments on the Flow of Water over Weirs.') Mémoires et Documents, Annales des Ponts et Chaussées, Paris, France, Sér. 7, Vol. 12, 2nd Sem., pp. 645-731 Plates (in French).

Bélanger, J.B. (1841). *Notes sur l'Hydraulique*. ('Notes on Hydraulic Engineering.') Ecole Royale des Ponts et Chaussées, Paris, France, session 1841-1842, 223 pages (in French).

Bos, M.G. (1976). *Discharge Measurement Structures*. Publication No. 161, Delft Hydraulic Laboratory, Delft, The Netherlands (also Publication No. 20, ILRI, Wageningen, The Netherlands).

Chanson, H. (2004). *The Hydraulics of Open Channel Flows: An Introduction*. Butterworth-Heinemann, Oxford, UK, 2nd edition, 630 pages.

Chanson, H. (2005). Physical modelling of the flow field in an undular tidal bore. *J. Hyd. Res.*, IAHR, Vol. 43, No. 3, pp. 234-244.

Chanson, H. (2006). Minimum Specific Energy and Critical Flow Conditions in Open Channels. *J. Irrig. and*

Drain. Eng., ASCE, Vol. 132, No. 5, pp. 498-502 (DOI: 10.1061/(ASCE)0733-9437(2006)132:5(498)).

Chanson, H. (2009). *Applied Hydrodynamics: An Introduction to Ideal and Real Fluid Flows*. CRC Press, Taylor & Francis Group, Leiden, The Netherlands, 478 pages.

Fawer, C. (1937). *Etude de Quelques Ecoulements Permanents à Filets Courbes*. ('Study of some Steady Flows with Curved Streamlines.') Thesis, Lausanne, Switzerland, Imprimerie La Concorde, 127 pages (in French).

Gonzalez, C.A., and Chanson, H. (2007). Experimental measurements of velocity and pressure distribution on a large broad-crested weir. *Flow Measurement and Instrumentation*, Vol. 18, No. 3-4, pp. 107-113 (DOI 10.1016/j.flowmeasinst.2007.05.005).

Henderson, F.M. (1966). *Open Channel Flow*. MacMillan Company, New York, USA.

Isaacs, L.T. (1981). *Effects of Laminar Boundary Layer on a Model Broad-Crested Weir*. Research Report No. CE28, Dept. of Civil Eng., Univ. of Queensland, Brisbane, Australia, 20 pages.

Liggett, J.A. (1993). Critical depth, velocity profiles and averaging. *J. of Irrig. and Drain. Eng.*, ASCE, Vol. 119, No. 2, pp. 416-422.

Liggett, J.A. (1994). *Fluid Mechanics.* McGraw-Hill, New York, USA.

Montes, J.S. (1998). *Hydraulics of Open Channel Flow*. ASCE Press, New-York, USA, 697 pages.

Montes, J.S., and Chanson, H. (1998). Characteristics of undular hydraulic jumps. Results and calculations. *J. Hydr. Eng.*, ASCE, Vol. 124, No. 2, pp. 192-205.

Ramamurthy, A.S., Tim, U.S., and Rao, M.V.J. (1988). Characteristics of square-edged and round-nosed broad-crested weirs. *J. of Irrig. and Drain. Eng.*, ASCE, Vol. 114, No. 2, pp. 61-73.

Sargison, J.E., and Percy, A. (2009). Hydraulics of broad-crested weirs with varying side slopes. *J. of Irrig. and Drain. Eng.*, ASCE, Vol. 135, No. 1, pp. 115-118.

Schlichting, H. (1979). *Boundary Layer Theory*. McGraw-Hill, New York, USA, 7th edition.

Serre, F. (1953). Contribution à l'etude des ecoulements permanents et variables dans les canaux. ('Contribution to the study of permanent and non-permanent flows in channels.') *J. La Houille Blanche*, Dec., pp. 830-872 (in French).

Tison, L.J. (1950). Le déversoir epais. ('Broad-Crested Weir.') *J. La Houille Blanche*, pp. 426-439 (in French).

Vierhout, M.M. (1973). *On the Boundary Layer Development in Round Broad-Crested Weirs with a Rectangular Control section*. Report No. 3, Lab.Hydraulics and Catchment Hydrology, Agricultural University, Wageningen, The Netherlands, 73 pages.

Vo, N.D. (1992). *Characteristics of Curvilinear Flow Past Circular-Crested Weirs*. Ph.D. thesis, Concordia Univ., Canada.

Woodburn, J.G. (1932). Tests of broad-crested weirs. *Transactions*, ASCE, Vol. 96, pp. 387-416. Discussion: Vol. 96, pp. 417-453.